

# A novel co-precipitation synthesis of a new phosphor $\text{Lu}_2\text{O}_3:\text{Eu}^{3+}$

Qiwei Chen<sup>a,b</sup>, Ying Shi<sup>a,\*</sup>, Liqiong an<sup>a</sup>, Shiwei Wang<sup>a</sup>,  
Jiyang Chen<sup>a,b</sup>, Jianlin Shi<sup>a</sup>

<sup>a</sup> Shanghai Institute of Ceramics, Chinese Academy of Sciences, Shanghai 200050, China

<sup>b</sup> Graduate School of the Chinese Academy of Sciences, Beijing 100039, China

Received 13 August 2005; received in revised form 5 January 2006; accepted 21 January 2006

Available online 23 March 2006

## Abstract

Europium-doped  $\text{Lu}_2\text{O}_3$  phosphors were prepared via a co-precipitation process. The influence of precipitants on morphology and dispersibility of the obtained  $\text{Lu}_2\text{O}_3$  powders were investigated. Precipitation was performed with three different precipitants, namely ammonium hydroxide ( $\text{NH}_3\cdot\text{H}_2\text{O}$ ), ammonium hydrogen carbonate ( $\text{NH}_4\text{HCO}_3$ ), and the mixture of  $\text{NH}_3\cdot\text{H}_2\text{O}$  and  $\text{NH}_4\text{HCO}_3$ . Ultrafine, nearly monodispersed, weakly agglomerated and near-spherical lutetia powders could be obtained with mixed  $\text{NH}_3\cdot\text{H}_2\text{O}$  and  $\text{NH}_4\text{HCO}_3$  as the precipitant. The precipitate precursor with the mixed precipitant was believed to possess a basic carbonate composition and its thermal decomposition and phase evolution processes were investigated. Photoluminescence characteristics of  $\text{Lu}_2\text{O}_3:\text{Eu}^{3+}$  phosphors obtained by this modified precipitation method were also studied. © 2006 Elsevier Ltd. All rights reserved.

**Keywords:** Optical properties;  $\text{Lu}_2\text{O}_3$ ; Precipitation; Phosphors

## 1. Introduction

Lutetium-based materials have attracted considerable attention as host crystals during the last 2 decades, among which Ce-doped  $\text{Lu}_2\text{SiO}_5$  and  $\text{LuAlO}_3$  have become the most competitive candidates to replace  $\text{Bi}_4\text{Ge}_3\text{O}_{12}$  in positron emission tomography (PET) cameras.<sup>1</sup> The crystallographic structure of  $\text{Lu}_2\text{O}_3$  is of the same type as cubic  $\text{Y}_2\text{O}_3$ .<sup>2</sup> In contrast, lutetium could be a more favorable cation than yttrium for lanthanide dopant emission.<sup>3</sup> Due to its high density ( $\sim 9.42 \text{ g/cm}^3$ ) and high Z-number of lutetium,  $\text{Lu}_2\text{O}_3$  can serve as a promising host material for some novel applications in electrooptics field. The crystal field of lutetia ceramics favors their uses as a host material in ceramic lasers or scintillators. Lutetia doped with Nd or Yb is a promising ceramic laser material,<sup>4,5</sup> while europium-doped  $\text{Lu}_2\text{O}_3$  ceramic scintillator can find its application in the field of X-ray imaging technology.<sup>6</sup>

Different synthesis methods lead to different particle morphologies and specific surface areas, which, in turn, determine the particle properties. Preparation of lutetia-doped with  $\text{Eu}^{3+}$

by the conventional ceramic powder processing is not favorable, as it employs a solid-state reaction of the oxides at high temperatures with sequential grinding and firing steps. It has been long recognized that wet-chemical process offers considerable advantages of good mixing of the starting material and excellent chemical homogeneity of the final product. As Robinson described,<sup>7</sup> the secret to improve a ceramic material is the control of the structure at very small length scales in an early stage of fabrication; chemistry might be the way to achieve this goal. Many chemical methods have been adopted to fabricate ultrafine lutetia powders. For example, Zych adopted combustion synthesis method to prepare nanostructured  $\text{Lu}_2\text{O}_3:\text{Eu}^{3+}$  phosphors,<sup>8</sup> moreover, oxalate precipitation<sup>6</sup> and a molten salts route<sup>9</sup> were employed by Lempicki and Trojan-Piegza to prepare  $\text{Lu}_2\text{O}_3:\text{Eu}^{3+}$  phosphors, respectively.

Co-precipitation has been verified its feasibility for fabricating ceramic powders with favorable characteristics. However, for rare earth oxides, two commonly used precipitants, oxalic acid and urea, were not adopted due to some of their disadvantages. For example, the relative high values of the solubility constants ( $K_{\text{sp}}$ ) of the rare earth oxalates will cause rapid and thorough reaction of the precipitation, thus resulting in a fast growing rate and uncontrolled severe agglomeration of the resultant crystallites; the considerably low hydrolyzation rate of

\* Corresponding author. Tel.: +86 21 52414905; fax: +86 21 52413903.  
E-mail address: [yshi@mail.sic.ac.cn](mailto:yshi@mail.sic.ac.cn) (Y. Shi).

urea limits the yield of homogeneous precipitation process. The aim of the present work is to synthesize nanostructured  $\text{Eu}^{3+}$ -doped  $\text{Lu}_2\text{O}_3$  phosphors with favorable characteristics using an improved co-precipitation method. The mixture of ammonium hydroxide ( $\text{NH}_3 \cdot \text{H}_2\text{O}$ ) and ammonium hydrogen carbonate ( $\text{NH}_4\text{HCO}_3$ ) is used as a mixed precipitant.  $\text{Lu}_2\text{O}_3:\text{Eu}^{3+}$  phosphors obtained by this modified co-precipitation processing show uniform and nanosized grains and its photoluminescence properties were also investigated.

## 2. Experimental

Lutetium and europium nitrate solution were prepared with corresponding oxide (purity > 99.9%, Rare Earth Products Ltd., Hongkong, China) dissolved in slightly excess nitric acid. The concentration of the  $\text{Eu}_2\text{O}_3$  dopant was set at 5 mol% and compensated by an equivalent decrease of the lutetium oxide. Analytical grade ammonium hydroxide and ammonium hydrogen carbonate were mixed to act as a mixed precipitant. For the purpose of comparison,  $\text{NH}_3 \cdot \text{H}_2\text{O}$  and  $\text{NH}_4\text{HCO}_3$  were also used individually. The precursor precipitate was produced by adding 250 ml of the precipitant solution ( $\sim 2.5$  M) at a speed of 3 ml/min into 1000 ml of the mother solution ( $\sim 0.06$  M for  $\text{Lu}^{3+}$ ) under mild stirring. The resultant suspension, after aged for 24 h, was filtered using a suction filter, washed four times with deionized water, and then twice with ethyl alcohol, and followed by drying at  $100^\circ\text{C}$  for 24 h. The dried precursor was crushed with an alumina pestle and mortar and calcined at  $550^\circ\text{C}$ ,  $650^\circ\text{C}$ ,  $750^\circ\text{C}$ ,  $850^\circ\text{C}$  and  $1000^\circ\text{C}$  for 2 h, respectively. Fig. 1 gives a flow chart describing relevant details of the co-precipitation processing.

Phase structure identification was performed with X-ray diffractometer (D/max 2550 V, Rigaku, Japan) utilizing nickel filtered Cu  $K\alpha$  radiation ( $1.5406 \text{ \AA}$ ) in the range of  $2\theta = 10\text{--}70^\circ$ . IR absorbance spectra were recorded using a Thermo Nicolet Nexus Fourier Transform infrared spectrometer with KBr

pellets. TG-DTA-MS measurements were conducted using a NETZSCH-STA 449C apparatus. Powder morphology and microstructure were observed by field-emission scanning electron microscopy (FESEM, JSM-6700F, JEOL, Japan). Specimens for the transmission electron microscopy (TEM, JEM2010 JEOL, Japan) study were ultrasonically dispersed into methanol, and the suspension was spread on the surface of silicon plate. Photoluminescence measurements were carried out on a fluorescence spectrometer (Fluorolog-3, Jobin Yvon, France) at room temperature.

## 3. Results and discussion

Fig. 2 shows the Fourier transform infrared (FTIR) absorption spectra of the dried precursor powders in the range  $4000\text{--}400 \text{ cm}^{-1}$ . In the case of  $\text{NH}_3 \cdot \text{H}_2\text{O}$  precipitant alone, though after many times of water washing and ethyl alcohol rinsing, residual  $\text{NO}_3^-$  and  $\text{NH}_4^+$  still exists. The intense absorption band at around  $1380 \text{ cm}^{-1}$  and the peak locating at  $1540 \text{ cm}^{-1}$  indicate the existences of  $\text{NO}_3^-$  and  $\text{NH}_4^+$ , respec-

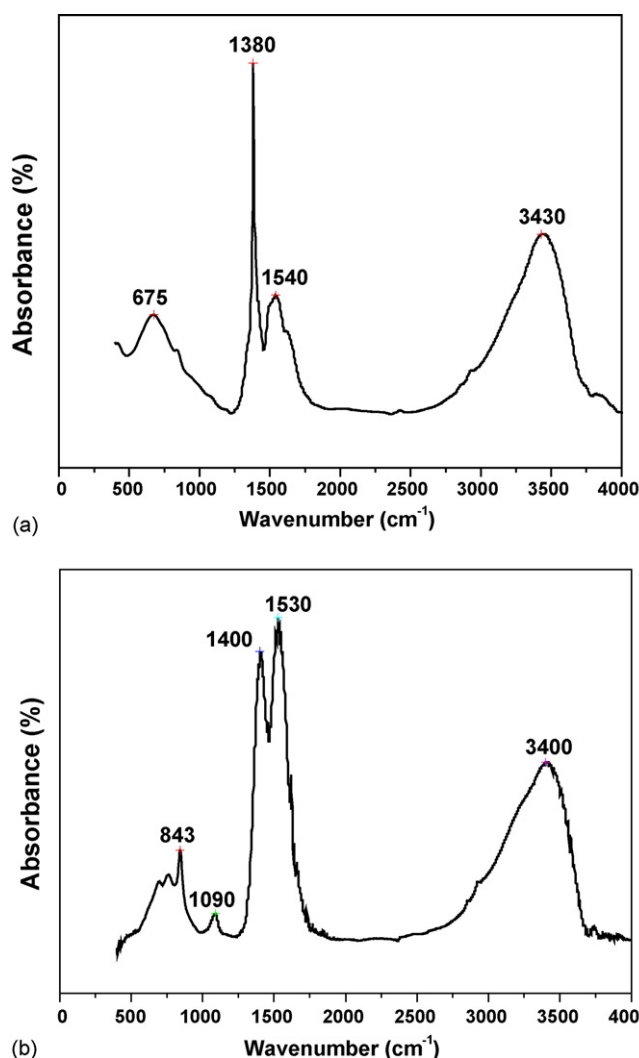


Fig. 2. FT-IR of the precursors prepared with: (a)  $\text{NH}_3 \cdot \text{H}_2\text{O}$ , (b)  $\text{NH}_4\text{HCO}_3$  or  $\text{NH}_3 \cdot \text{H}_2\text{O} + \text{NH}_4\text{HCO}_3$  as the precipitants.

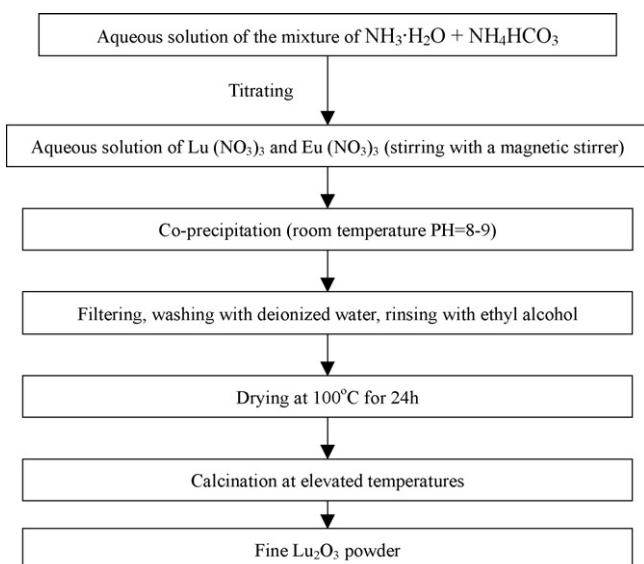


Fig. 1. Flow chart illustrating sequence used in the precipitation experiments.

tively. IR spectra of the two precursors prepared with single  $\text{NH}_4\text{HCO}_3$  and with  $\text{NH}_3 \cdot \text{H}_2\text{O} + \text{NH}_4\text{HCO}_3$  mixture are almost identical. The peak at around  $750\text{ cm}^{-1}$  results from deformation of O–H band. The broad absorption band at  $3410\text{ cm}^{-1}$  is assigned to O–H stretching. The two intense peaks at  $1530\text{ cm}^{-1}$  and  $1400\text{ cm}^{-1}$  are assigned to the asymmetric stretch of C–O in  $\text{CO}_3^{2-}$ , while the absorption peaks at  $1090\text{ cm}^{-1}$  and  $840\text{ cm}^{-1}$  are due to the symmetric stretch of C–O band and deformation vibration of C–O in  $\text{CO}_3^{2-}$ , respectively. These absorption peaks indicate the presence of carbonate groups.

TEM morphologies of the precipitate precursors obtained by the three precipitants are shown in Fig. 3(a), (b) and (c).

The resultant powders from  $\text{NH}_3 \cdot \text{H}_2\text{O}$  are severely agglomerated. The primary particles are aggregated together and almost no discrete particles can be seen from the photographs. Severe agglomeration of the  $\text{NH}_3 \cdot \text{H}_2\text{O}$  method was due to the bridging of the adjacent particles with water by hydrogen bonding and the huge capillary force generated during drying.<sup>10</sup> Readey<sup>11</sup> proposed that this hydroxide process involves hydrogen bonding of surface hydroxyl groups on the hydroxide precipitate, and the water molecules can bridge the surface hydroxyl groups of neighbouring precipitates, thus bonding adjacent particles. Powders synthesized by the  $\text{NH}_4\text{HCO}_3$  method, though apparently agglomerated, show a lower agglomeration degree than that of

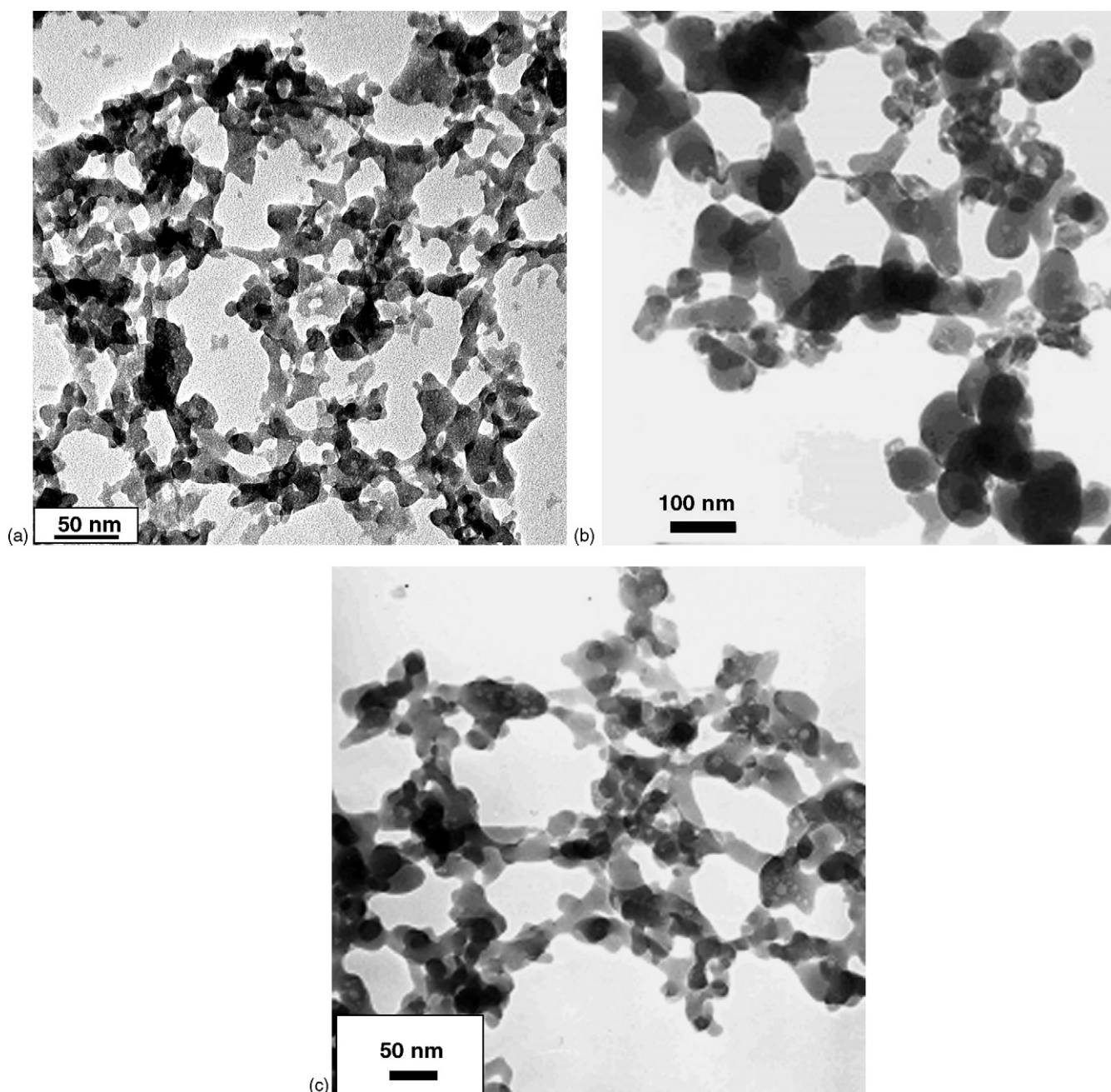


Fig. 3. TEM photographs of the precipitate precursors prepared with: (a)  $\text{NH}_3 \cdot \text{H}_2\text{O}$ , (b)  $\text{NH}_4\text{HCO}_3$  and (c)  $\text{NH}_3 \cdot \text{H}_2\text{O} + \text{NH}_4\text{HCO}_3$  as the precipitants.

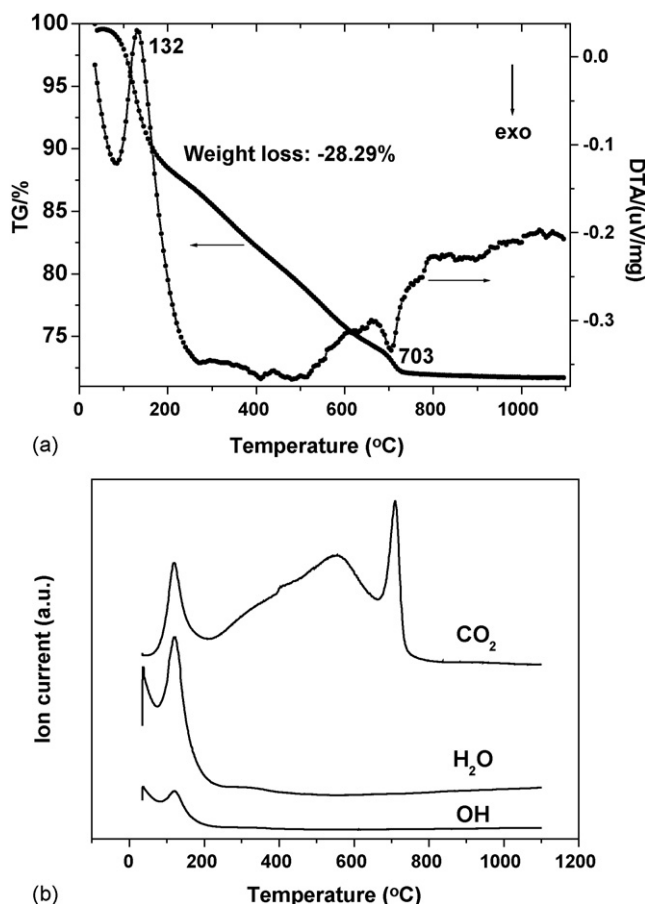
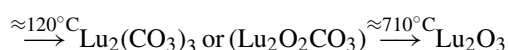
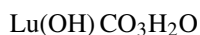


Fig. 4. (a) TG-DTA and (b) MS curves of the precursors prepared with  $\text{NH}_3 \cdot \text{H}_2\text{O} + \text{NH}_4\text{HCO}_3$  as the precipitant.

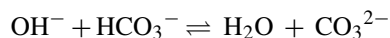
the hydroxide-derived powders. The basic carbonate precipitates precursor from the mixed precipitant method show better dispersibility and weaker agglomeration. Relatively discrete, spherical particles only slightly link together. The precursor morphology favors the creation of well-dispersed oxide powders after calcination.

TG-DTA curves of the precursor produced by the mixed precipitant method are given in Fig. 4(a). The TG curve displays a relatively continuous weight loss to near 800 °C. The total weight loss is around 28.3%. The DTA curve shows an endothermic peak at about 132 °C corresponding to the release of water of hydration and OH, and the exothermic peak at about 703 °C due to the chemical decomposition of the carbonate or dioxycarbonate, which is indicated by the MS curves shown in Fig. 4(b). The weight loss of the sample between 100 °C and 800 °C is apparently a consequence of the thermal decomposition of  $\text{Lu}(\text{OH})\text{CO}_3\text{H}_2\text{O}$  into  $\text{Lu}_2\text{O}_3$ , according to the following equation:



The precipitation process is somewhat similar to that of urea homogeneous precipitation. The homogeneous decomposition of urea and subsequent dissociation of the reaction products will

yield  $\text{OH}^-$  and  $\text{CO}_3^{2-}$ .<sup>12</sup> Composition of the precursor obtained by the mixed precipitant technique will be the result of the competition between  $\text{OH}^-$  and the carbonate species to form precipitates with  $\text{Lu}^{3+}$  as characterized by the following chemical reactions:



XRD patterns of the precursor prepared with  $\text{NH}_3 \cdot \text{H}_2\text{O} + \text{NH}_4\text{HCO}_3$  and  $\text{Lu}_2\text{O}_3$  powders calcined at various temperatures from 550 °C to 1000 °C are illustrated in Fig. 5. The as-precipitated powder is amorphous with no XRD peaks. The crystallization process of the precipitate precursor with subsequent heat-treatment can be clearly seen. Calcination at 550 °C is not adequate for the precursor to crystallize. After calcined at 650 °C for 2 h, the precursor transforms to cubic  $\text{Lu}_2\text{O}_3$  phase. The diffraction peaks intensity enhance and also the full-width at half-maximum (FWHM) reduce due to the improvement of crystallinity and grain growth upon further heating to 850 °C and 1000 °C.

Fig. 6(a)–(c) show the SEM morphologies of the lutetia powders by calcining the precipitates at 1000 °C for 2 h with  $\text{NH}_3 \cdot \text{H}_2\text{O}$ ,  $\text{NH}_4\text{HCO}_3$  and  $\text{NH}_3 \cdot \text{H}_2\text{O} + \text{NH}_4\text{HCO}_3$  mixture as precipitants, respectively. The lutetia powders obtained from the mixed precipitant are much better dispersed than those from  $\text{NH}_3 \cdot \text{H}_2\text{O}$  and  $\text{NH}_4\text{HCO}_3$  as precipitants. Narrowly distributed in size, weakly agglomerated and fine spherical powders can be obtained by the mixed precipitant method after calcined at 1000 °C for 2 h. The average crystallites sizes of lutetia powders prepared with  $\text{NH}_3 \cdot \text{H}_2\text{O} + \text{NH}_4\text{HCO}_3$  method calcined at

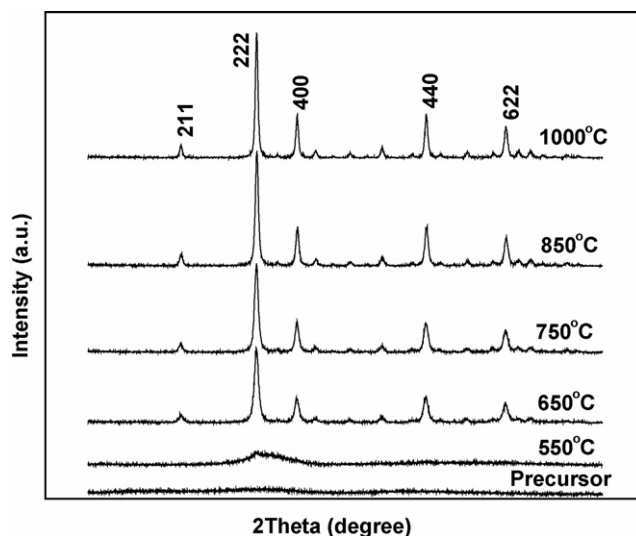


Fig. 5. XRD patterns of the precursor prepared with  $\text{NH}_3 \cdot \text{H}_2\text{O} + \text{NH}_4\text{HCO}_3$  as the precipitant.



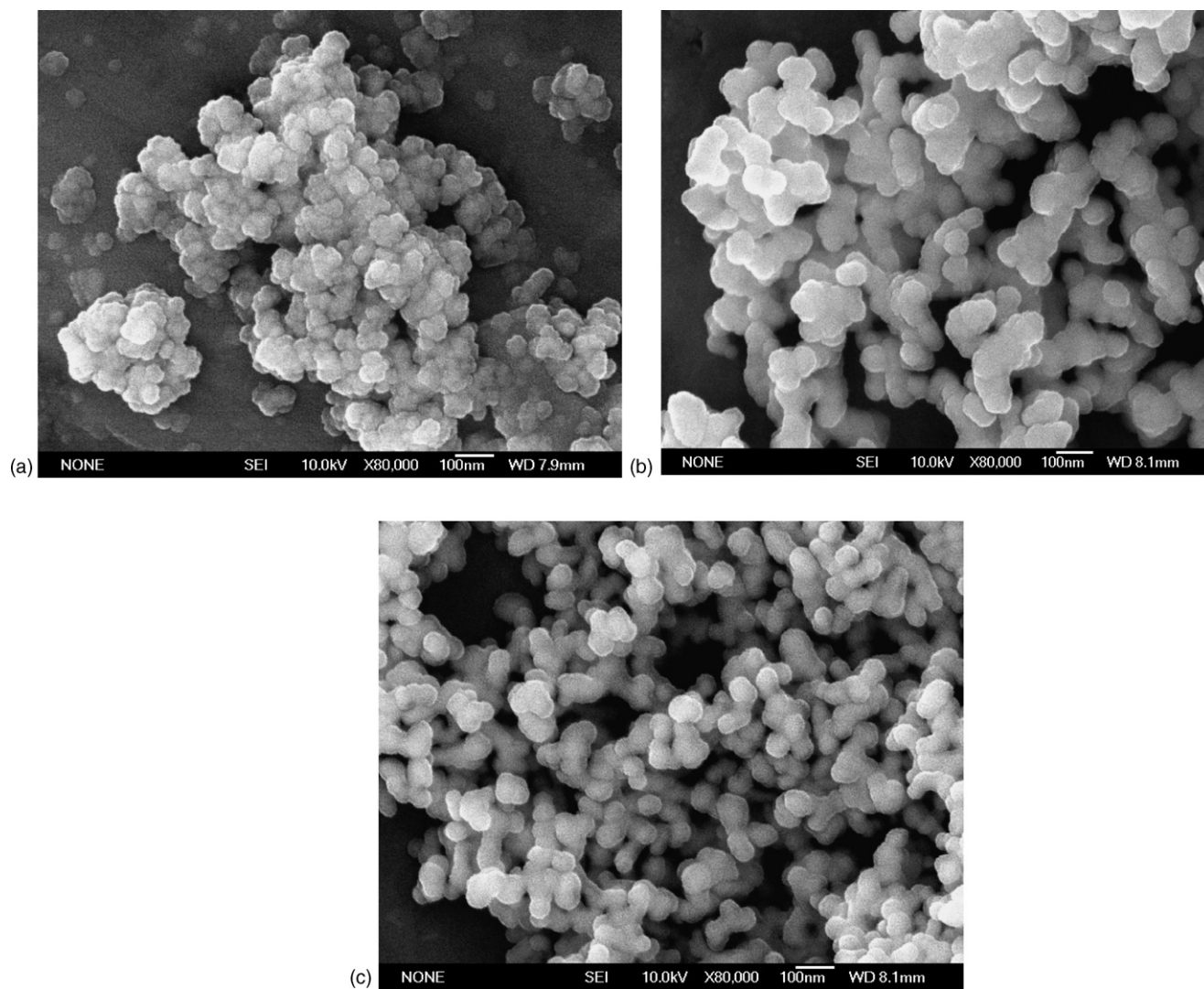


Fig. 6. SEM morphologies of powders calcined at 1000 °C for 2 h with: (a)  $\text{NH}_3 \cdot \text{H}_2\text{O}$ , (b)  $\text{NH}_4\text{HCO}_3$  and (c)  $\text{NH}_3 \cdot \text{H}_2\text{O} + \text{NH}_4\text{HCO}_3$  as the precipitants.

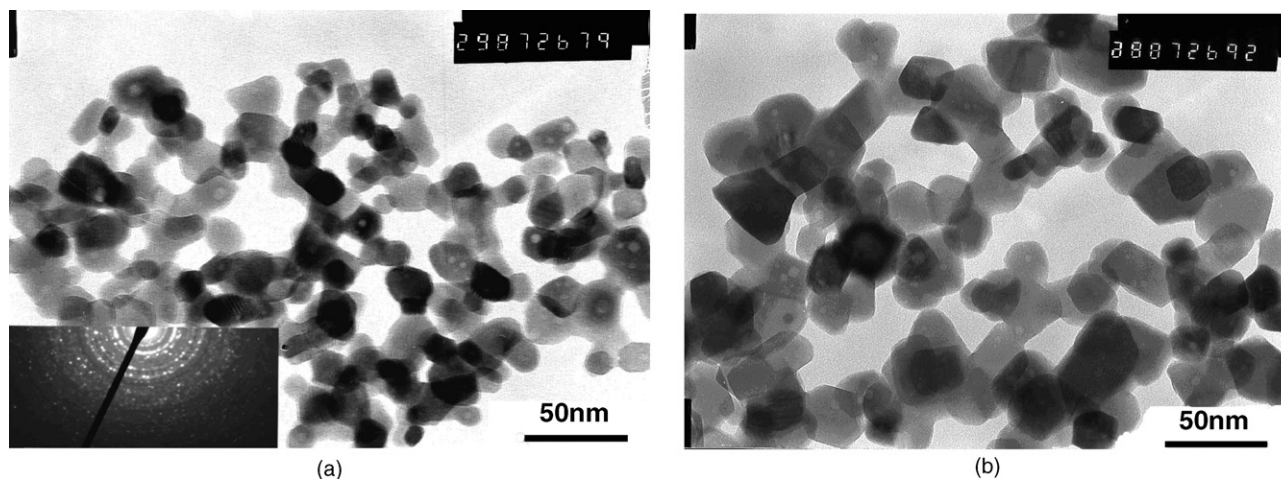


Fig. 7. TEM micrographs of lutetia powders prepared with  $\text{NH}_3 \cdot \text{H}_2\text{O} + \text{NH}_4\text{HCO}_3$  calcined at: (a) 850 °C for 2 h (SAED inset) and (b) 1000 °C for 2 h.

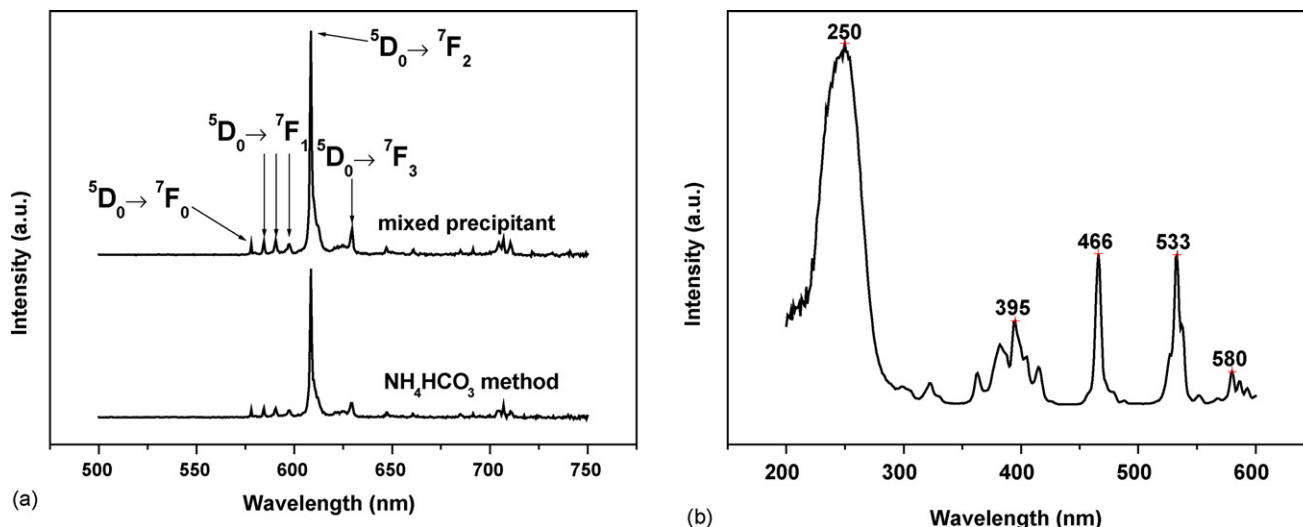


Fig. 8. (a) Emission ( $\lambda_{\text{ex}} = 394 \text{ nm}$ ) spectra of the phosphors from  $\text{NH}_4\text{HCO}_3$  and the mixed  $\text{NH}_3 \cdot \text{H}_2\text{O} + \text{NH}_4\text{HCO}_3$  precipitants; (b) excitation ( $\lambda_{\text{em}} = 610 \text{ nm}$ ) spectrum of the phosphors from mixed  $\text{NH}_3 \cdot \text{H}_2\text{O} + \text{NH}_4\text{HCO}_3$  precipitant.

850 °C and 1000 °C for 2 h are about 20 nm and 40 nm, respectively, which were revealed by TEM micrographs as shown in Fig. 7(a) and (b). Selected area electron diffraction (SAED) of the powders calcined at 850 °C indicates complete crystallization. The  $\text{Lu}_2\text{O}_3$  powder obtained at 1000 °C experiences significant grain growth. From the powder morphology comparison, it is suggested that the introduction of  $\text{CO}_3^{2-}$  is essential to obtain less agglomerated and uniformly dispersed powders. The release of  $\text{CO}_2$  during the decomposition of the carbonate will prevent the particles from severe agglomerating with each other, thus resulting in well-dispersed nanopowders.

Fig. 8(a) shows the emission ( $\lambda_{\text{ex}} = 394 \text{ nm}$ ) spectra of the phosphors obtained from  $\text{NH}_4\text{HCO}_3$  and the mixed precipitant techniques. We choose the two phosphor samples for comparison purpose because they have similar powder characters such as grain size, particle morphology and surface state. The emission spectra demonstrate the well-known  $^5\text{D}_0 \rightarrow ^7\text{F}_j$  ( $j = 0, 1, 2 \dots$ ) transition of  $\text{Eu}^{3+}$  ions. The energy level diagram of  $\text{Eu}^{3+}$  in  $\text{Lu}_2\text{O}_3$  host is shown in Fig. 9. The irradiation with ultraviolet (UV) light of nanocrystalline  $\text{Lu}_2\text{O}_3:\text{Eu}^{3+}$  into the charge transfer band, which yields intense red emission at 610 nm dominated by  $^5\text{D}_0 \rightarrow ^7\text{F}_2$  transition. It has been proposed that phosphors materials with fine crystallite size, narrow size distribution, non-agglomerated feature, and spherical morphology have good luminescent properties.<sup>13</sup>  $\text{Lu}_2\text{O}_3:\text{Eu}^{3+}$  phosphors obtained by the mixed precipitant processing show enhanced photoluminescence compared with that from the  $\text{NH}_4\text{HCO}_3$  method. This is probably due to the near-spherical particle morphology and relatively good particle dispersion with high particle size uniformity from the mixed precipitant technique. Fig. 8(b) shows the excitation ( $\lambda_{\text{em}} = 610 \text{ nm}$ ) spectrum of the phosphors obtained from  $\text{NH}_3 \cdot \text{H}_2\text{O} + \text{NH}_4\text{HCO}_3$  method. The broad excitation band in the region between 220 nm and 280 nm is known to result from the charge-transfer (CT) transitions between  $\text{O}^{2-}$  and  $\text{Eu}^{3+}$  ions, which corresponds to the electronic transition from the  $2p$  orbital of  $\text{O}^{2-}$  to the  $4f$  orbital of  $\text{Eu}^{3+}$ .<sup>14</sup> The narrow lines in visible and near UV part of the excitation spectrum reflect the intraconfigu-

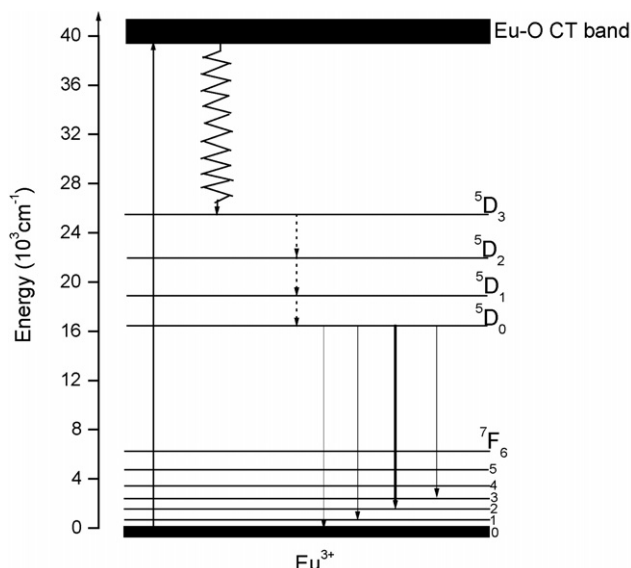


Fig. 9. Energy level diagram of  $\text{Eu}^{3+}$  in  $\text{Lu}_2\text{O}_3$  host lattice.

rational partially forbidden  $4f \rightarrow 4f$  transitions within the  $\text{Eu}^{3+}$  ion.<sup>15</sup>

#### 4. Conclusions

Europium-doped lutetium oxide phosphors have been prepared by a novel co-precipitation method, with  $\text{NH}_3 \cdot \text{H}_2\text{O} + \text{NH}_4\text{HCO}_3$  mixture as the precipitant. Ultrafine, nearly monodispersed, weakly agglomerated and spherical powders can be obtained. The combined analysis results of IR, TG-DTA and MS characterizations reveal that the precursor has a basic carbonate composition and its thermal decomposition process includes the removals of hydration water,  $\text{OH}^-$  and  $\text{CO}_3^{2-}$  ions during heating-up. Phosphors obtained by this mixed precipitant technique present enhanced photoluminescence due to its favorable powder characteristics.

## Acknowledgement

This work was financially supported by the National Natural Science Foundation of China (No. 50572115).

## References

1. Lempicki, A. and Glodo, J., Ce-doped scintillators: LSO and LuAP. *Nucl. Instrum. Meth. A*, 1998, **416**, 333–344.
2. Hanic, F., Hartmanová, M., Knab, G. G., Urusovskaya, A. and Bagdasarov, K. S., Real structure of undoped  $\text{Y}_2\text{O}_3$  single crystals. *Acta Cryst.*, 1984, **B40**, 76–82.
3. Boyer, J. C., Vetrone, F., Capobianco, J. A., Speghini, A. and Bettinelli, M., Variation of fluorescence lifetimes and Judd-Ofelt parameters between  $\text{Eu}^{3+}$  doped bulk and nanocrystalline cubic  $\text{Lu}_2\text{O}_3$ . *J. Phys. Chem. B*, 2004, **108**(52), 20137–20143.
4. Lu, J., Takaichi, K., Uematsu, T., Shirakawa, A., Musha, M., Ueda, K., Yagi, H., Yanagitani, T. and Kaminskii, A. A., Promising ceramic laser material: highly transparent  $\text{Nd}^{3+}:\text{Lu}_2\text{O}_3$  ceramic. *Appl. Phys. Lett.*, 2002, **81**, 4324–4326.
5. Griebner, U., Petrov, V., Petermann, K. and Peters, V., Passively mode-locked  $\text{Yb}:\text{Lu}_2\text{O}_3$  laser. *OPT. EXPRESS*, 2004, **12**, 3125–3130.
6. Lempicki, A., Brecher, C., Szupryczynski, P., Lingertat, H., Nagarkar, V. V., Tipnis, S. V. and Miller, S. R., A new lutetia-based ceramic scintillator for X-ray imaging. *Nucl. Instrum. Meth. Phys. Res. A*, 2002, **488**, 579–590.
7. Robinson, A. L., A chemical route to advanced ceramics. *Science*, 1986, **233**, 25–27.
8. Zych, E., Hreniak, D. and Strek, W., Spectroscopy of Eu-doped  $\text{Lu}_2\text{O}_3$ -based X-ray phosphor. *J. Alloys Comp.*, 2002, **341**, 385–390.
9. Trojan-Piegza, J. and Zych, E., Preparation of nanocrystalline  $\text{Lu}_2\text{O}_3:\text{Eu}$  phosphor via a molten salts route. *J. Alloys Comp.*, 2004, **380**, 118–122.
10. Kaliszewski, M. S. and Heuer, A. H., Alcohol interaction with zirconia powders. *J. Am. Ceram. Soc.*, 1990, **73**(6), 1504–1509.
11. Readey, M. J., Lee, R. R., Halloran, J. W. and Heuer, A. H., Processing and sintering of ultrafine  $\text{MgO-ZrO}_2$  and  $(\text{MgO}, \text{Y}_2\text{O}_3)\text{-ZrO}_2$  powders. *J. Am. Ceram. Soc.*, 1990, **73**(6), 1499–1503.
12. Sordelet, D. J., Akinc, M., Panchula, M. L., Han, Y. and Han, M. H., Synthesis of yttrium aluminum garnet precursor powders by homogeneous precipitation. *J. Eur. Ceram. Soc.*, 1994, **14**(2), 123–130.
13. Kang, Y. C., Roh, H. S. and Park, S. B., Preparation of  $\text{Y}_2\text{O}_3:\text{Eu}$  phosphor particles of filled morphology at high precursor concentrations by spray pyrolysis. *Adv. Mater.*, 2002, **12**, 451–453.
14. Blasse, G. and Grabmeier, B. C., How does a luminescent material absorb its excitation energy? In *Luminescent Materials*. Springer-Verlag, Berlin, 1994. pp. 9–32.
15. Blasse, G. and Bril, A., Photoluminescence efficiency of phosphors with electronic transitions in localized centers. *J. Electrochem. Soc.*, 1968, **115**, 1067–1075.